THE JOURNAL OF BIOLOGICAL CHEMISTRY VOL. 287, NO. 19, pp. 15923–15934, April 4, 2012

Involvement of Polo-like Kinase 1 (Plk1) in Mitotic Arrest by Inhibition of Mitogen-activated Protein Kinase-Extracellular Signal-regulated Kinase-Ribosomal S6 Kinase 1 (MEK-ERK-RSK1) Cascade*[S]

Received for publication, October 11, 2011, and in revised form, January 28, 2012 Published, JBC Papers in Press, March 16, 2012, DOI 10.1074/jbc.M111.312413

Ran Li[‡], Dian-Fu Chen[‡], Rong Zhou[‡], Sheng-Nan Jia[‡], Jin-Shu Yang[‡], James S. Clegg[§], and Wei-Jun Yang[‡1]

From the [‡]Key Laboratory of Conservation Biology for Endangered Wildlife of the Ministry of Education and College of Life Sciences, Zhejiang University, Hangzhou 310058, China and [§]Section of Molecular and Cellular Biology and Bodega Marine Laboratory, University of California, Davis, Bodega Bay, California 94923

Background: Plk1 can be inhibited by RSK1 during meiosis.
Results: Activities of members of the MEK-ERK-RSK1 signaling pathway increase when Plk1 is knocked down, and both of these pathways shut down during cell cycle arrest.
Conclusion: Plk1 inhibits the activity of RSK1 via a feedback signal transduction mode during mitosis.
Significance: We show that Plk1 is involved in G_2/M transition by inhibiting the RSK1 pathway.

Cell division is controlled through cooperation of different kinases. Of these, polo-like kinase 1 (Plk1) and p90 ribosomal S6 kinase 1 (RSK1) play key roles. Plk1 acts as a G_2/M trigger, and RSK1 promotes G_1 progression. Although previous reports show that Plk1 is suppressed by RSK1 during meiosis in *Xenopus* oocytes, it is still not clear whether this is the case during mitosis or whether Plk1 counteracts the effects of RSK1. Few animal models are available for the study of controlled and transient cell cycle arrest. Here we show that encysted embryos (cysts) of the primitive crustacean *Artemia* are ideal for such research because they undergo complete cell cycle arrest when they enter diapause (a state of obligate dormancy). We found that Plk1 suppressed the activity of RSK1 during embryonic mitosis and that Plk1 was inhibited during embryonic diapause and mitotic arrest. In addition, studies on HeLa cells using Plk1 siRNA interference and overexpression showed that phosphorylation of RSK1 increased upon interference and decreased after overexpression, suggesting that Plk1 inhibits RSK1. Taken together, these findings provide insights into the regulation of Plk1 during cell division and *Artemia* diapause cyst formation and the correlation between the activity of Plk1 and RSK1.

Polo-like kinases (Plks)[2] are a family of serine/threonine kinases that have emerged as vital regulators of many cellular events, including bipolar spindle formation, activation of Cdc2, and responses to DNA damage. The *Plk* gene was first identified during screening of *Drosophila* for mutants defective in cell division. Four polo family members are present in mammalian cells: Plk1, Plk2/Snk, Plk3/Fnk/Prk, and Plk4/Sak. All of these members contain a conserved C-terminal amino acid sequence termed the polo box domain, which provides a docking site for certain proteins (1), and a kinase domain, which is predicted to activate many protein kinases, including Aurora A/B, PKA, ERK1/2, RSK1/2, Akt/PKB, and MEK1 (2). The polo family members have largely non-overlapping functions; for example, Plk2 acts during entry into S phase (3–5), whereas Plk3 regulates several stress response pathways (6–9).

Compared with its homologs, Plk1 (and its associated signaling pathway) has attracted much attention because overexpression of Plk1 is tightly correlated with carcinogenesis (10, 11). Moreover, inhibition of Plk1 using RNA interference (RNAi) or specific small molecule inhibitors causes growth arrest or apoptosis in cancer cells (12–14). Plk1 activity is regulated by the upstream kinase Aurora A. Phosphorylation of amino acid Thr-210 (located within the kinase domain of Plk1) by Aurora A activates Plk1, enabling cells to complete entry into mitosis (15, 16). During *Xenopus* embryonic mitosis, Plx1 (*Xenopus* polo-like kinase) forms a stable complex with Myt1, a membrane-associated kinase belonging to the Wee1 family, and acts as a negative regulator of Cdc2 (17–19), inhibiting Myt1 and promoting the G_2/M transition (20). However, during *Xenopus* oocyte maturation when hormonal stimulation exists, Myt1 can also be phosphorylated by p90 ribosomal S6 kinase (p90RSK; also known as RSK) (20). Thus, Myt1 acts as a common substrate for RSK1 in meiosis and Plk1 in mitosis.

There are six phosphorylation sites in RSK1 that are critical for its activation and its subsequent role in substrate phosphorylation (21, 22). Of these, phosphorylation of Ser-380 is important for RSK1 activation, driving functions such as regulation of gene expression and protein synthesis, and cell cycle regulation as a downstream kinase in the Mos-MAPK pathway (23). During *Xenopus* oocyte maturation, RSK both phosphorylates and

* This work was supported by the National Natural Sciences Foundation of China (Grants 40876069 and 40730212) and the National Basic Research Program of China (973 Program Grant 2010CB833803).
[S] This article contains supplemental Figs. S1 and S2.
The nucleotide sequence(s) reported in this paper has been submitted to the GenBank™/EBI Data Bank with accession number(s) JN021275 and JN021276.
[1] To whom correspondence should be addressed. Tel.: 86-571-88273176; Fax: 86-571-88273176; E-mail: w_jyang@cls.zju.edu.cn.
[2] The abbreviations used are: Plk, polo-like kinase; RSK1, p90 ribosomal S6 kinase 1; Cdc2, cell division control protein 2; Myt1, a dual specificity protein kinase; L:D, hours light:hours dark; dsRNA, double-stranded RNA; CSF, cytostatic factor.

down-regulates Myt1, causing prophase I arrest (24). Degradation of Mos inactivates p90RSK when mature metaphase II-arrested oocytes are fertilized (25–27), and Myt1 forms a complex with Plk1. Therefore, it would be interesting to examine the control mechanism of cell cycle progression in which RSK1 affects Myt1 in meiosis and Plk1 affects Myt1 in mitosis. Studies conducted at different time points during the progression from oocyte to embryo suggest that RSK1 and Plk1 share a close relationship. RSK1 inhibits the effects of Plk1-Myt1 interactions, and previous studies indicate that MEK1/2 and ERK1/2 are phosphorylated in Plk1-depleted cells (28); however, it is still not clear whether Plk1 interacts with RSK1 and/or how this pathway operates.

Plk1 is an essential regulator of the cell cycle during both meiosis and mitosis; however, commonly used animal models are limited in that cell cycle arrest must be induced by treatment with drugs. That is not the case in the crustacean *Artemia* used in the present study. Maternal females can produce either nauplius larvae by direct development or encysted embryos (cysts) that enter diapause, a state of obligate dormancy, at the gastrula stage. Diapause embryos do not undergo cell division or DNA synthesis (29) and remain in total cell cycle arrest. Even when diapause is terminated, the postdiapause embryos continue cell cycle arrest until larvae are produced (29–31).

In the present study, we showed that Plk1 and RSK1 were inactivated in diapause cysts but were highly active in nauplius larvae in which cell division resumed. Because Plk1 and RSK1 play important roles during mitosis, this result suggests a mechanism by which mitosis can be shut down during cyst formation. In addition, the knockdown of Plk1 increased the activation of RSK1 in *Artemia* oocytes and embryos. Furthermore, overexpression of Plk1 in HeLa cells resulted in decreased activation of RSK1. The interplay between these two molecules was controlled by the upstream MEK-ERK pathway and was not simply due to their common downstream substrate, Myt1.

EXPERIMENTAL PROCEDURES

Animals—Cysts of parthenogenetic *Artemia* from Gahai, a highland salt lake in Qinghai province of China (37° 9′ 22″ north, 97° 34′ 7″ east), were a gift from Prof. Feng-Qi Liu (College of Life Sciences, Nankai University, Tianjin, China). Cysts were hatched, and larvae were raised to adults in 8% artificial seawater (Blue Starfish, Hangzhou, Zhejiang, China) at 28 °C and fed once every 2 days with *Chlorella* powder. The daily light regime (hours light:hours dark) determines the reproductive mode in these animals (32). Under 16L:8D, nauplius larvae are produced and released. Under 4L:20D, encysted gastrula embryos (cysts) are released. We define stages 1–6 as developmental stages: stage 1, oocytes in the ovaries, residing there for about 3 days; stage 2, oocytes in the oviducts, lasting for about 3 h; and stages 3–6, embryos that have been developing in the ovisac (uterus) for 1, 2, 3, and 4 days, respectively (31).

Molecular Cloning of Artemia Plk1 and Aurora cDNAs—A specific fragment of *Artemia* Plk1-encoding cDNA sequence was isolated as described by Dai *et al.* (33). Full-length cDNA was achieved using the FirstChoice™ RLM-RACE kit (Ambion, Austin, TX) through 3′ and 5′ rapid amplification of cDNA ends with gene-specific primers (5R1, 5R2, 3F1, and 3F2 in Table 1). The Aurora A-encoding cDNA was obtained through two rounds of degenerate PCR (using primers AF1, AF2, AR1, and AR2 in Table 1). Afterward, the full-length cDNA was achieved through 3′ and 5′ rapid amplification of cDNA ends with gene-specific primers (A3F1, A3F2, A3F3, A5R1, and A5R2 in Table 1). The sequences of both of these genes were imported into SeqMan of Lasergene software (DNASTAR, Madison, WI). Then the complete cDNAs and the deduced peptides were determined using Blastn and Blastx, respectively, on the NCBI web site. The nucleotide sequences of Plk1- and Aurora A-encoding cDNAs were submitted to GenBank™ under accession numbers JN021275 and JN021276.

Real Time PCR—Total RNA was extracted from lateral pouches and ovisacs filled with oocytes or embryos in adults that had been injected with double-stranded RNA (dsRNA) and in animals carrying different developmental stages using TRIzol reagent (Invitrogen). Reverse transcription was then performed, and the single-stranded cDNAs were used as templates for real time PCR. PCRs were performed using SYBR® Premix Ex Taq™ (TaKaRa, Shiga, Japan) on the Bio-Rad MiniOpticon™ Real-Time PCR System with specific primers, QF and QR (Table 1). Using α-tubulin mRNA as the internal control (with primers TubulinF and TubulinR; Table 1), the relative transcript levels between the GFP RNAi group and the Plk1 RNAi group as well as in different development stages were analyzed by the comparative CT method as described by Schmittgen and Livak (34). Each group had three independent repetitions, and the data are expressed as means ± S.E. The differences were considered significant for $p < 0.01$ by a two-tailed, paired Student's *t* test.

dsRNA Synthesis and Microinjection—Reconstructed plasmids that contained two inverted T7 polymerase sites flanking the cloning region were obtained (named pET-T7) as described previously (30). Next, a 442-bp fragment including the 5′-UTR and parts of the 5′ coding region of the *Plk1* gene and a fragment of the *Aurora A* gene were both amplified by PCR with primers iF and iR and primers AiF and AiR, respectively (Table 1). These amplified fragments were excised using XbaI and NcoI and subcloned into pET-T7. For the negative control, a 359-bp GFP cDNA fragment was amplified from pcDNA3.1/CT-GFP-TOPO® plasmid (Invitrogen) (using primers GiF and GiR; Table 1) and subcloned into pET-T7 at the same restriction sites. This recombinant plasmid was used to express dsRNA of GFP, *Artemia* Plk1, and Aurora A. After transformation into *Escherichia coli* DH5α, inserted nucleotide sequences of the recombinant plasmids were confirmed by DNA sequencing. Recombinant plasmids were then transformed into *E. coli* HT115, and the dsRNAs were purified as described by Yodmuang *et al.* (35).

Artemia microinjection was performed using the Ultra-MicroPump II equipped with the Micro4™ MicroSyringe pump controller (World Precision Instruments, Sarasota, FL). In initial dose-response experiments, we injected 1, 0.8, 0.5, or 0.1 μg of dsRNA per individual adult at the instar XII stage. We chose 1 μg per adult as the injection dose in other experiments to be described.

Cells and Transfection—HeLa cells were cultured in Dulbecco's modified minimum essential medium (Invitrogen) supple-

TABLE 1

Nucleotide sequences and positions of primers used in polymerase chain reactions

The underlined regions represent the recognition sequences of the restriction endonucleases. RF and RR and TubulinF and TubulinR were designed according to the cDNA sequences under GenBank accession numbers EF427895.1 and AF078670.1, respectively. R, reverse; F, forward.

Primer	Length	Position	Direction	Sequence (5′–3′)
	bp			
5R1	23	493–515	R	ACCTAACTTCAAATCTCTATGGA
5R2	23	443–465	R	CTCCGATAAGAATCTGTCGTAAG
3F1	20	523–542	F	TTTTGAATGACGAAATGGAA
3F2	20	392–411	F	GGAACTCCACAAGCGACGA
AF1	20	178–197	F	GGNAARTTYGGNAAYGTNTA
AF2	20	194–203	F	TTYGGNAAYGTNTAYYTNGC
AR1	20	571–590	R	CANCCRAARTCNGCDATYTT
AR2	20	526–545	R	ARRTTYTCNGGYTTDATRTC
A3F1	20	274–293	F	TGTGAACATCAACTGCGACG
A3F2	20	390–409	F	TGCTGCTAATGGAGAGATGT
A3F3	20	902–921	F	TCTGGGTGCTCAAACTTCTC
A5R1	20	483–502	R	GGCAGTATTTCAAGGCATCT
A5R2	20	311–329	R	ATTGGGGTGCCTGAGATGAC
GiF	30	122–144	F	GCTCTAGAAACTTACCCTTAATTTTATTTGC
GiR	28	461–480	R	CATGCCATGGGCCATTCTTTGGTTTGTCTC
iF	26	57–74	F	GCTCTAGAATGTCTAGTCGCAGTGAT
iR	28	448–465	R	CATGCCATGGCTCCGATAAGAATCTGTC
AiF	25	158–174	F	GCTCTAGATTGGAAAACCTCTTGGC
AiR	26	642–660	R	GGAATTCCATTTCAGGTGGCAGATAG
QF	21	65–85	F	TCGCAGTGATAGACCTGAGCC
QR	21	201–221	R	TTTGCCAGCCAGTATTTCGTT
TubulinF	20	446–465	F	GCAGTGGTCTACAAGGTTTC
TubulinR	22	774–795	R	ATCAAAACGAAGGCTGGCGGTG
PF	32	55–77	F	CCCAAGCTTTCATGTCTAGTCGCAGTGATAGA
PR	30	1767–1787	R	CGCGGATCCTTAATCACTCTTTCCTTGTTG
RF	33	109–130	F	CCCAAGCTTTCATGCCACTTGCAAATTTGCAAG
RR	32	2231–2253	R	CGCGGATCCTCACTTCACAGAGCCAAGTTCGG

mented with 10% calf serum (Invitrogen) and incubated in a 5% CO_2 environment at 37 °C.

siRNAs were synthesized according to the manufacturer's instructions for the *in vitro* transcription T7 kit (for siRNA synthesis) (TaKaRa, code number D6140). The targeting sequences of human *Plk1* (NCBI Reference Sequence accession number NM_005030.3) were siRNA1 (AAGGGCGGCTTT-GCCAAGTGCTT) and siRNA2 (AATGAATACAGTATTC-CCAAGCA), corresponding to the coding regions 181–203 and 796–818 relative to the start codon. Control siRNA was designed by scrambling Plk1 siRNA1. Then Plk1 and control siRNA were transfected into HeLa cells using Lipofectamine 2000 reagent (Invitrogen) according to the manufacturer's instructions. Cells were harvested and analyzed 24–48 h after transfection.

The pEGFP-C1 vector was used for construction of the pEGFP-Plk1 and pEGFP-RSK1 plasmids. Cloned *Artemia* Plk1 and RSK1 fragments (using primers PF and PR and primers RF and RR; Table 1) were inserted into the multiple cloning sites between HindIII and BamHI. For transient transfection, HeLa cells were transfected with these recombinant expression plasmids and pEGFP-C1 vector as a blank control using Lipofectamine 2000 transfection reagent (Invitrogen) according to the manufacturer's instructions.

Cell Synchronization and Cell Cycle Analysis—HeLa cells were synchronized and harvested at different phases according to the method described previously (36). Briefly, 4 mM thymidine was added to the medium when cells reached 50% confluence. After 18 h of incubation, thymidine was washed off and replaced with normal medium. Then after 10 h of incubation, cells were treated with 4 mM thymidine again for another 18 h. Finally, thymidine was removed with normal medium, and cells were harvested every 2 h (up to 12 h).

Cell cycle analysis was carried out using flow cytometry. Fixed cells were treated with RNase A (100 μg/ml; Sigma) and stained for 40 min with propidium iodine (50 μg/ml; Sigma) at 4 °C. Cell cycle phase analysis was performed in a Beckman Coulter flow cytometer (FC500MCL).

Western Blotting Analysis—Protein samples were obtained using TRIzol reagent (Invitrogen) after RNA extraction for real time PCR. Proteins were applied to 10% SDS-polyacrylamide gels for electrophoresis and transferred to PVDF membranes (Millipore, Billerica, MA) using standard methods. Membranes were blocked for 1 h at room temperature in 1% blocking buffer and probed overnight at 4 °C with the following antibodies: anti-phospho-Plk1 (phospho-Plk1 Thr-210; 1:1000; Abcam, Cambridge, MA), anti-phospho-RSK (phospho-p90RSK Ser-380; 1:1000; Cell Signaling Technology, Beverly, MA), anti-RSK (rabbit anti-pan-RSK; 0.5 μg/ml; R&D Systems, Minneapolis, MN), anti-MAPK (p44/42 mitogen-activated protein kinase; 1:1000; Cell Signaling Technology), anti-MEK1/MEK2 (Ser(P)-218/222; 1:1000; Epitomics, Burlingame, CA), anti-Myt1 (1:1000; Cell Signaling Technology), anti-Plk1 raised in rabbits (1:1000; HuaAn Biotechnology, Hangzhou, Zhejiang, China), and anti-Aurora raised in rabbits (1:1000; HuaAn Biotechnology). After washing twice with 20 mM Tris (pH 8.2), 150 mM NaCl, 0.05% Tween 20 (TBST) and blocking using a Western blotting kit (Roche Applied Science), the membranes were incubated with peroxidase-labeled goat anti-rabbit/mouse IgG for 1 h in blocking buffer. After washing with TBST, membranes were processed for chemiluminescence detection using the BM Chemiluminescence Western Blotting kit (Roche Applied Science) and Eastman Kodak Co. film according to the manufacturer's instructions.

Immunofluorescence of HeLa Cells—HeLa cells were incubated with siRNA for 36 h on coverslips and then fixed for

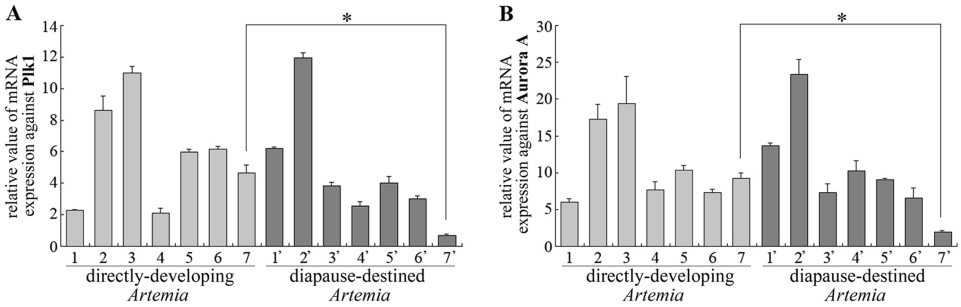

FIGURE 1. **Expression pattern of *Artemia Plk1* (*A*) and *Aurora A* (*B*) during development.** *Lanes 1–7* (*light gray*) correspond to samples from directly developing *Artemia*. *Lane 1*, oocytes residing in the ovaries; *lane 2*, oocytes in the oviducts; *lanes 3–6*, 1–4 days, respectively, after the oocytes entered the uterus; *lane 7*, released nauplius larva. Corresponding samples were obtained from diapause-destined *Artemia* (*lanes 1′–6′*; *dark gray*). *Lane 7′*, released diapause cysts. Results shown represent means ± S.E. * represents $p < 0.05$.

immunofluorescent staining. Cells were fixed with 4% formaldehyde overnight and then washed with phosphate-buffered saline (PBS). Fixed cells were blocked in antibody dilution buffer (PBS, 0.25% Triton X-100, 1% bovine serum albumin), and all subsequent staining was performed in the same buffer. The cells were labeled with α-tubulin antibody (Epitomics) for 2 h followed by incubation with a secondary FITC-conjugated antibody for 1.5 h. DNA was stained by incubation with DAPI for 30 min at room temperature.

Cell Death Assessment by DNA Fragmentation Assays—After injection of double-stranded RNAs, control and test group *Artemia* were gently homogenized in lysis buffer, and the somatic cells in the homogenate were assayed for internucleosomal DNA fragmentation according to the manufacturer's instructions (Cell Death Detection ELISA Plus kit, Roche Applied Science).

The TdT-mediated dUTP nick end labeling (TUNEL) assay was used to detect apoptosis as described by the manufacturer (DeadEnd™ Colorimetric TUNEL System, Promega, Madison, WI). On the 3rd day after embryos had first entered the ovisac, the adult *Artemia* were injected with dsRNAs, embedded in paraffin, and cut into 8-μm sections for TUNEL detection. Negative controls were generated by replacing TdT with distilled H_2O during the labeling step.

RESULTS

Molecular Characterization of Plk1 and Aurora A—As mentioned, *Artemia* were reared under light regimes that would produce swimming larvae (long day) or encysted embryos (short day). To understand the mechanisms underlying diapause cyst formation, a suppression-subtractive hybridization library of parthenogenetic *Artemia* was constructed in which double-stranded cDNAs from ovisacs of cyst-producing animals were used as testers, and those from the direct development pathway were used as drivers (33). The results (Figs. 1*A* and 2) showed that the *Plk1* gene was differentially expressed in these *Artemia*; in diapause-destined oocytes, the *Plk1* gene was down-regulated. The full-length Plk1 sequence was obtained using rapid amplification of cDNA ends and then analyzed (supplemental Fig. S1). The *Plk1* open reading frame comprised 1731 nucleotides and encoded a protein of 576 amino acids with a predicted molecular mass of 66 kDa. The deduced amino acid sequence showed that *Artemia* Plk1 comprised one kinase domain followed by two typical polo box domains. The protein also contained the typical Plk1 phosphorylation site (Thr-210; supplemental Fig. S1B). Supplemental Fig. S1B shows the amino acid sequence of *Artemia* Plk1 aligned with that of the polo gene from *Drosophila* and Plk from *Caenorhabditis elegans*, mouse, and human. Phylogenetic analysis was performed by the method of Hanks and Hunter (37) to compare the amino acid sequence of *Artemia* Plk1 (supplemental Fig. S1C) with those of other species.

Aurora A, encoded by a 1713-bp cDNA, contained 334 amino acids with a predicted molecular mass of 38 kDa (supplemental Fig. S2A). Supplemental Fig. S2B shows the amino acid sequence of *Artemia* Aurora A aligned with the aurora genes from *Drosophila*, *C. elegans*, mouse, and human. Phylogenetic analysis was performed to compare the amino acid sequence of *Artemia* Aurora A with those of other species (supplemental Fig. S2C). The genes for these two *Artemia* proteins shared no apparent homology with any other known genes or proteins in the DDBJ/EMBL/GenBank database.

Prior to nauplius or cyst formation, the paired oocytes pass from the ovaries to the oviducts and then into the ovisac (uterus) where they continue to develop over the next 4–5 days when cysts or larvae are released. Expression of the *Plk1* and *Aurora A* genes was characterized by real time PCR. Fig. 1 shows differences in expression of the *Plk1* (*A*) and *Aurora A* (*B*) genes in different developmental stages of both pathways. In the direct development pathway, the expression levels of both genes increased during oocyte maturation and then reached a peak at 1 day (*lane 3*) after the oocytes had entered the uterus. Subsequently, the expression of both genes decreased to lower levels that were maintained through development to and release of nauplius larvae (*lane 7*). In the case of the diapause-destined pathway, Plk1 and Aurora A expression was highest when the oocytes resided in the oviducts (*lane 2′*) and then decreased when these embryos were actively undergoing cell division (*lanes 3′–6′*). However, in diapause cysts released on the 4th day (*lane 7′*), the expression of both genes was much lower than in any other stage, notably when compared with the released nauplius larvae (*lane 7*). These results suggest that the reduced expression of Plk1 and Aurora A may be essential prerequisites leading to diapause cyst formation.

Plk1 Plays Leading Role during Artemia Embryo Development and Diapause Cyst Formation—Immunoblotting was performed next to evaluate the kinases in the Aurora A-Plk and

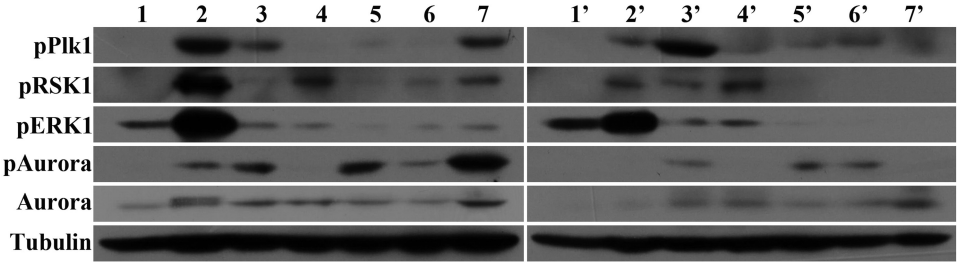

FIGURE 2. **Activation of Plk1, Aurora A, RSK1, and ERK in different stages in reproduction by two developmental pathways.** *Lanes 1–7* contain samples from directly developing *Artemia*. *Lane 1*, oocytes in the ovaries; *lane 2*, oocytes in the oviducts; *lanes 3–6*, 1–4 days, respectively, after the oocytes entered the ovisac; *lane 7*, swimming nauplii. Corresponding samples were obtained from stages leading to the production of diapause cysts (*lanes 1′–6′*). *Lane 7′*, released diapause cysts.

ERK-RSK1 pathways in both developmental routes. In oocytes programmed to develop into nauplii, the phosphorylation of Plk1 and RSK1 was maximal during the period when the oocytes resided in the oviduct (Fig. 2, *lane 2*). However, activation levels of both Plk1 and RSK1 are quite low during the oocyte maturation period in diapause-destined embryos (Fig. 2, *lane 1′*). In addition, the high activation of these kinases (Fig. 2, *lane 7*) in nauplius larvae compared with diapause cysts (Fig. 2, *lane 7′*) indicated again that these molecules play an important role in determining which developmental pathway will be taken as well as strictly controlling the cell cycle.

However, after this period of oocyte maturation in directly developing *Artemia*, the phosphorylation of both Plk1 and RSK1 decreased once the oocytes were deposited into the ovisac (Fig. 2, *lane 3*), the time when vigorous embryonic cell division begins. Note that in the 1st and 2nd days of embryonic cell division (Fig. 2, *lanes 3* and *4*), their activation patterns differed. Plk1 retained some activation at the 1st day after the beginning of embryo cell division (Fig. 2, *lane 3*) but decreased its activation the next day (Fig. 2, *lane 4*). However, RSK1 showed much lower activation at the 1st day after the beginning of cell division (Fig. 2, *lane 3*) but increased its activation the next day (Fig. 2, *lane 4*). Similarly, during this same period in the diapause-destined *Artemia*, the variations in their activation levels showed a trend similar to that in directly developing *Artemia*. At the 1st day after the beginning of embryonic cell division (Fig. 2, *lane 3′*), the phosphorylation of Plk1 reached a peak but sharply declined the next day (Fig. 2, *lane 4′*). However, RSK1 showed much lower phosphorylation at the 1st day after the beginning of embryonic cell division (Fig. 2, *lane 3′*) but increased its activation to the maximal level the next day (Fig. 2, *lane 4*). These results demonstrated the alternative role of Plk1 and RSK1 in the regulation of the embryonic mitosis.

Depletion of Plk1 Inhibits Mitosis and Simultaneously Activates Kinases Involved in MEK-ERK-RSK1 Pathway—dsRNA designed from the Plk1 cDNA sequence was injected into the body cavity of adult *Artemia* just before ovarian development. Dose-response analysis showed that at 2 days before the formation of the diapause gastrula (observed about 2 weeks postinjection) Plk1 protein expression levels decreased with increasing doses of Plk1 dsRNA (Fig. 3*A*). Injection of 1 μg of dsRNA per individual *Artemia* resulted in low levels of Plk1 (Fig. 3*A*). A study of dsRNA effects over time was also carried out. Injection of 1 μg of dsRNA per individual was carried out using the immature adult instar XII stage. RNAi efficiency was evaluated at the 1st, 3rd, and 4th days after the oocytes had entered the ovisac. As shown in Fig. 3, most endogenous Plk1 in the test group was knocked down compared with the control group.

Oocytes and embryos were next stained with DAPI (Fig. 3*C*). In the GFP RNAi group, the embryos began to divide 6 h after the oocytes had entered the ovisac (Fig. 3*C*, *column 2*), and mitosis continued for the next 4 days (Fig. 3*C*, *columns 5–8*). Nauplii were released on the 5th day as shown in Fig. 3*C*, *column 9*. In contrast, embryos in the Plk1 RNAi group showed no evidence of cell division throughout development and release.

To address the function of Plk1 during embryonic cell division and its effects on the MEK-ERK-RSK1 signaling pathway, the kinases involved in each pathway were examined by immunoblotting (Fig. 3*A*). An antibody to phosphohistone 3 was used to confirm whether cell division was occurring normally in the embryos. As expected, the test group displayed much less phosphohistone 3 than the control group during mitosis, reflecting a defect in mitosis caused by knockdown of Plk1. Meanwhile, the level of RSK1 phosphorylation and that of its upstream kinases MEK and ERK increased. Myt1, a common substrate for both Plk1 and RSK1, was also detected. Although RSK1 was activated, Myt1 was less inhibited compared with the control group, suggesting that Plk1, rather than RSK1, acted as the major regulator of Myt1 during mitosis. Taken together, these results indicate that the interplay between RSK1 and Plk1 is most probably regulated by upstream kinases involved in the RSK1 signaling pathway rather than by a simple effect through their common substrate, Myt1.

To confirm that full activation of the MEK-ERK-RSK1 cascade was mediated by Plk1, Aurora A, which acts as the upstream kinase of Plk1, was also used as a target for RNAi. Immunoblotting showed that Aurora A protein expression decreased markedly after RNAi treatment (Fig. 3*B*). The phosphorylation levels of the kinases were also examined as described above with similar results (Fig. 3*A*). In *Artemia* depleted of Aurora A, the phosphorylation level of Plk1 decreased. In addition, the main members in the ERK pathway, including MEK, ERK, and RSK1, showed an increased level of activation, whereas phosphorylation of Myt1 and histone 3 both decreased. These results give strong support to our view described previously that inhibition of the Aurora A-Plk1 pathway leads to the overall activation of the MEK-ERK-RSK pathway.

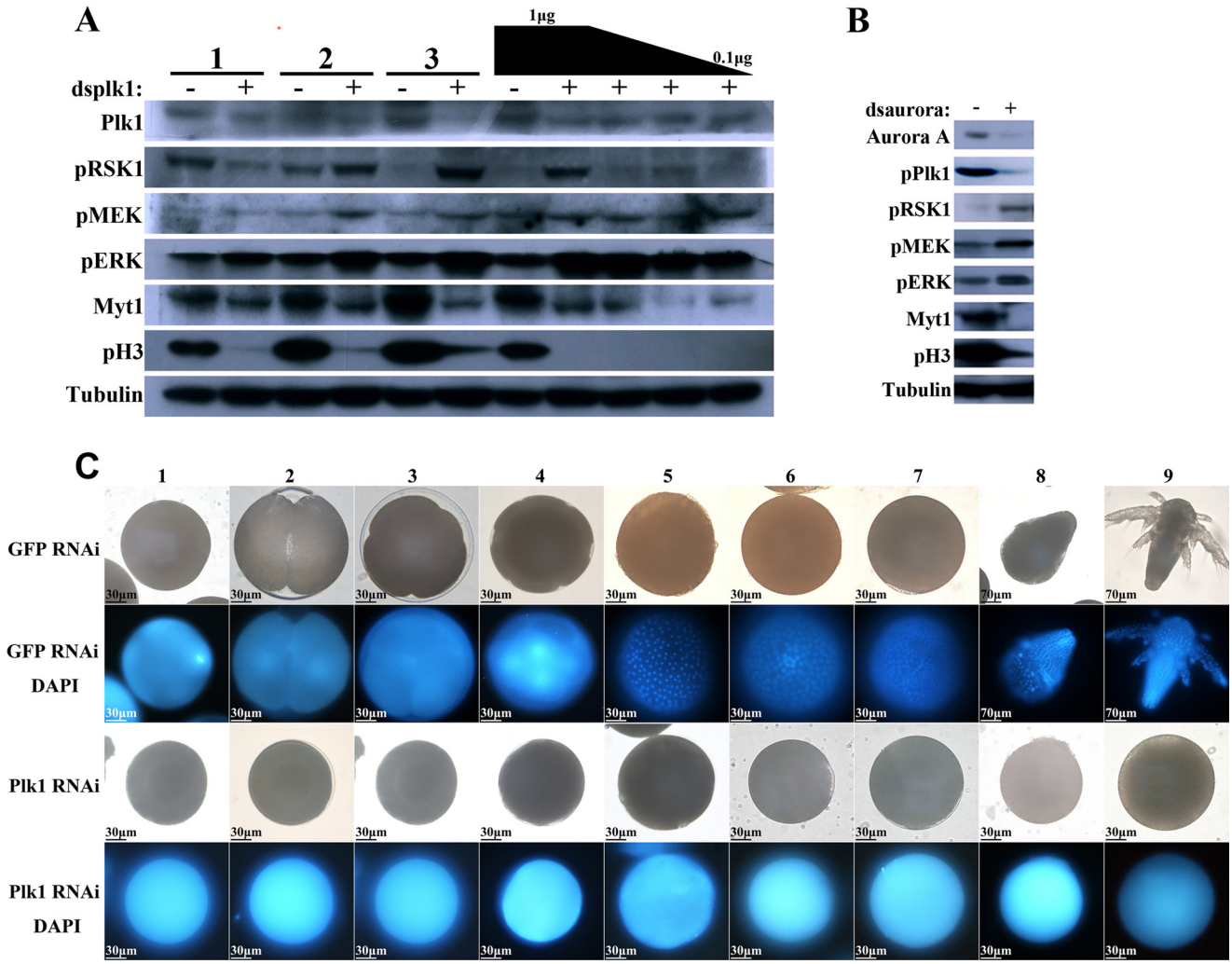

FIGURE 3. **Gene knockdown of Plk1 and Aurora A by RNAi in *Artemia*.** *A* and *B*, expression and phosphorylation (*p*) status of Plk1 and RSK1 using *Artemia* injected with GFP dsRNA (−), Plk1 dsRNA (+), and Aurora dsRNA (*B*). *Lanes 1*, *2*, and *3* contain samples obtained 1, 2, and 4 days after the oocytes entered the ovisac, respectively. The *black trapezoid* represents dsRNA doses of 1, 0.8, 0.5, and 0.1 μg per individual maternal adult. *C*, embryos from Plk1 RNAi-treated *Artemia* that did not undergo cell division. *Column 1*, oocytes after entry to the oviducts; *columns 2*, *3*, and *4*, oocytes after 6, 8, and 12 h in the ovisac, respectively; *columns 5–8*, oocytes at 1–4 days after they entered the ovisac, respectively; *column 9*, nauplii released by the GFP RNAi group (*top*) and the pseudo-cysts formed by the Plk RNAi group (*bottom*). *pH3*, phosphohistone 3.

RNAi Treatment of Plk1 Induces Formation of Pseudo-diapause Cysts—To further investigate the role of Plk1 during mitosis, adults were injected with Plk dsRNA. Morphological observation revealed that *Artemia* injected with Plk1 dsRNA and maintained under 16L:8D conditions produced what we refer to here as pseudo-diapause cysts (Fig. 4*A*) rather than nauplii released by the control groups (Fig. 4*B*). Trypan blue stained the pseudo-diapause cysts (Fig. 4*C*) but not normal cyst controls (Fig. 4*D*), indicating the death of pseudo-diapause cysts. In addition, *Artemia* injected with Plk1 dsRNA and maintained under 4L:20D conditions produced abnormal, deformed cysts (Fig. 4, *E* and *G*) compared with the diapause cysts produced by the control groups (Fig. 4, *F* and *H*), suggesting that developmental failure results from the lack of Plk1. The efficiency of dsRNA interference, monitored using semiquantitative PCR and real time PCR, revealed that the level of Plk1 mRNA was less than 30% of that in controls (Fig. 4*I*).

Plk1 Effects RSK1 in HeLa Cells in Manner Similar to That in Artemia—Interaction between the Plk1 and RSK1 signaling pathways was examined in human cells to determine whether the relationship was the same as that observed in *Artemia*. Using the method of double thymidine block (36), HeLa cells were synchronized at the G_1/S boundary, and then thymidine was removed using ordinary medium to enable cells to progress through the cell cycle. Cells were harvested subsequently every 2 h (up to 12 h) after release from arrest, and the levels of Plk1, Aurora A, and RSK1 were monitored by immunoblotting as cells progressed through the cell cycle (Fig. 5*A*). The results showed that during a complete cell cycle Plk1 began to be phosphorylated at G_2 phase, stayed at a high activation level in M phase, and began to be dephosphorylated gradually when cells completed mitosis and entered G_1 phase. However, during the critical M phase period when Plk1 executes its control function, the activation level of RSK1 declined to a lower level than that during early G_1 and G_2 phases. Then after M phase, the activa-

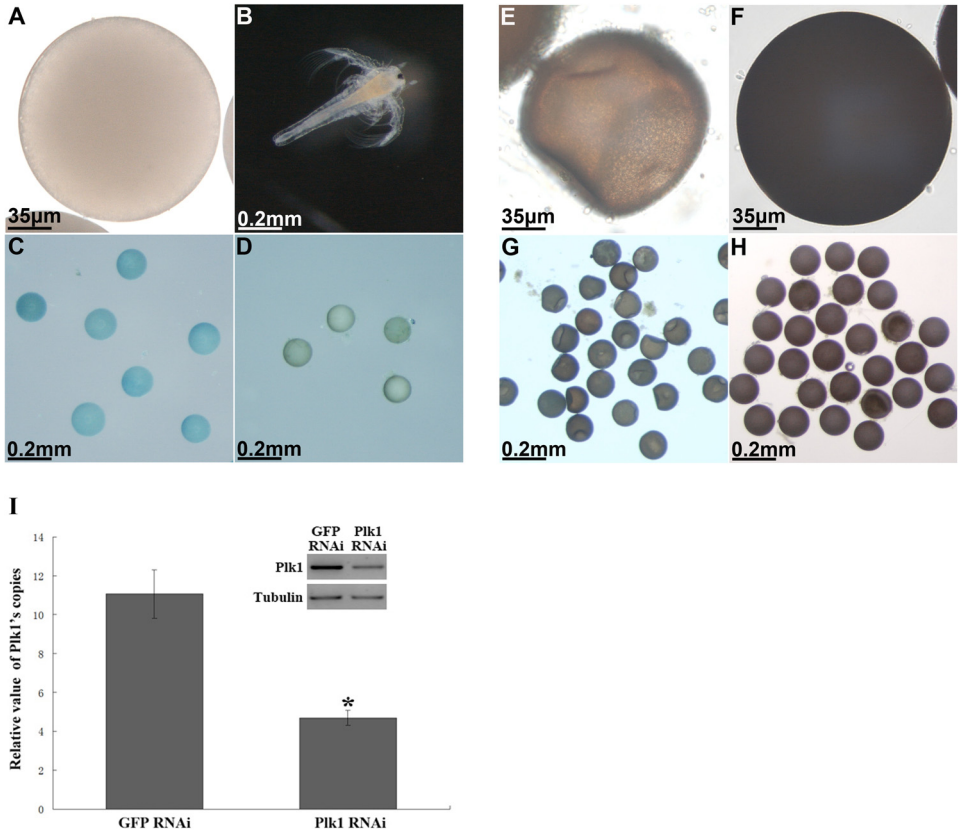

FIGURE 4. **Morphology of *Artemia* injected with GFP and Plk1 dsRNAs under different L:D regimes.** *A*, white transparent oocyte produced by the Plk1 RNAi-treated group. *B*, nauplius from the control group. *C*, pseudo-cysts laid by the Plk1 RNAi-treated group stained by trypan blue. *D*, normal diapause cyst not stained by trypan blue. *E* and *G*, deformed cysts laid by the Plk1 RNAi-treated group under a short photoperiod. *F* and *H*, opaque cysts laid by the control group maintained under the same conditions as in *E* and *G*. *I*, detection of relative Plk1 transcript levels in the control and test groups by real time PCR. All data represent the mean ± S.E. * indicates a significant difference ($p = 0.0036$) by one-way analysis of variance.

tion of RSK1 recovered, although RSK1 showed no activation in late G_1 and early S phases (Fig. 5*A*).

Next, HeLa cells were transfected with two designed siRNAs targeting the human *Plk1* gene or a scrambled siRNA as a control followed by immunoblotting. The results showed that both Plk1 siRNAs successfully knocked down expression of the *Plk1* gene (Fig. 5*B*). In addition, the morphology of the siRNA-transfected HeLa cells observed after staining for tubulin showed a number of abnormalities, including multiple spindle poles, multiple polo chromosomes, and multiple nuclei, all typical characteristics of Plk1-depleted cells (Fig. 5*C*). Strikingly, the phosphorylation of endogenous RSK1 increased after exposure to Plk1 siRNA relative to that seen in the control group.

Because Plk1 inhibits RSK1 during mitosis, the corresponding influence of RSK1 on Plk1 was also examined. A specific inhibitor of RSK1, SL0101 (Tocris, Ellisville, MO), was added to the HeLa cell culture medium. Immunoblotting showed that the inhibitor successfully suppressed the phosphorylation of RSK1 24 h after treatment but had only a small effect if any on the phosphorylation of Plk1 (Fig. 5*D*).

To confirm the interrelationship between Plk1 and RSK1, HeLa cells were transfected with GFP-fused Plk1 or RSK1. Fluorescence microscopy revealed the intracellular localization of these two exogenous proteins, showing that GFP-fused Plk1 was distributed throughout the cell, whereas GFP-fused RSK1 localized to the cytoplasm (Fig. 6*A*). Immunoblotting showed that at 24 and 48 h after transfection the activation level of endogenous RSK1 had decreased along with the expression and activation of exogenous Plk1 (Fig. 6*B*). Also at 24 and 48 h after transfection, in GFP-fused RSK1 transfected cells, endogenous phospho-Plk1 increased along with expression and activation of exogenous RSK1. At the same times, endogenous phospho-RSK1 decreased. Note that activation of exogenous RSK1 only appeared at 24 h after transfection; however, the decreased phosphorylation level of endogenous RSK1 remained stable at both 24 and 36 h after transfection in step with dephosphorylation of endogenous Plk1.

Inhibition of Both Plk1 and RSK1 Increased Apoptosis in Artemia and HeLa Cells—To determine the condition of cells after knockdown of Plk1 and to explore the role of RSK1 activation, dsRNA interference and apoptosis detection assays were performed using adult *Artemia*. The results showed that interference with dsPlk1, dsRSK1, and both dsPlk1 and RSK1 decreased phosphorylation of the corresponding target molecules compared with the control group (Fig. 7*A*, *bottom left*). The phosphorylation level of RSK1 and ERK increased in Plk1 RNAi *Artemia*, consistent with the results given above. Myt1 was less inhibited in all three test groups, but the reduction in the RSK1 RNAi group was not as obvious as that in the Plk1 RNAi group. In double RNAi *Artemia*, the phosphorylation level change of ERK and Myt1 was close to that seen with the

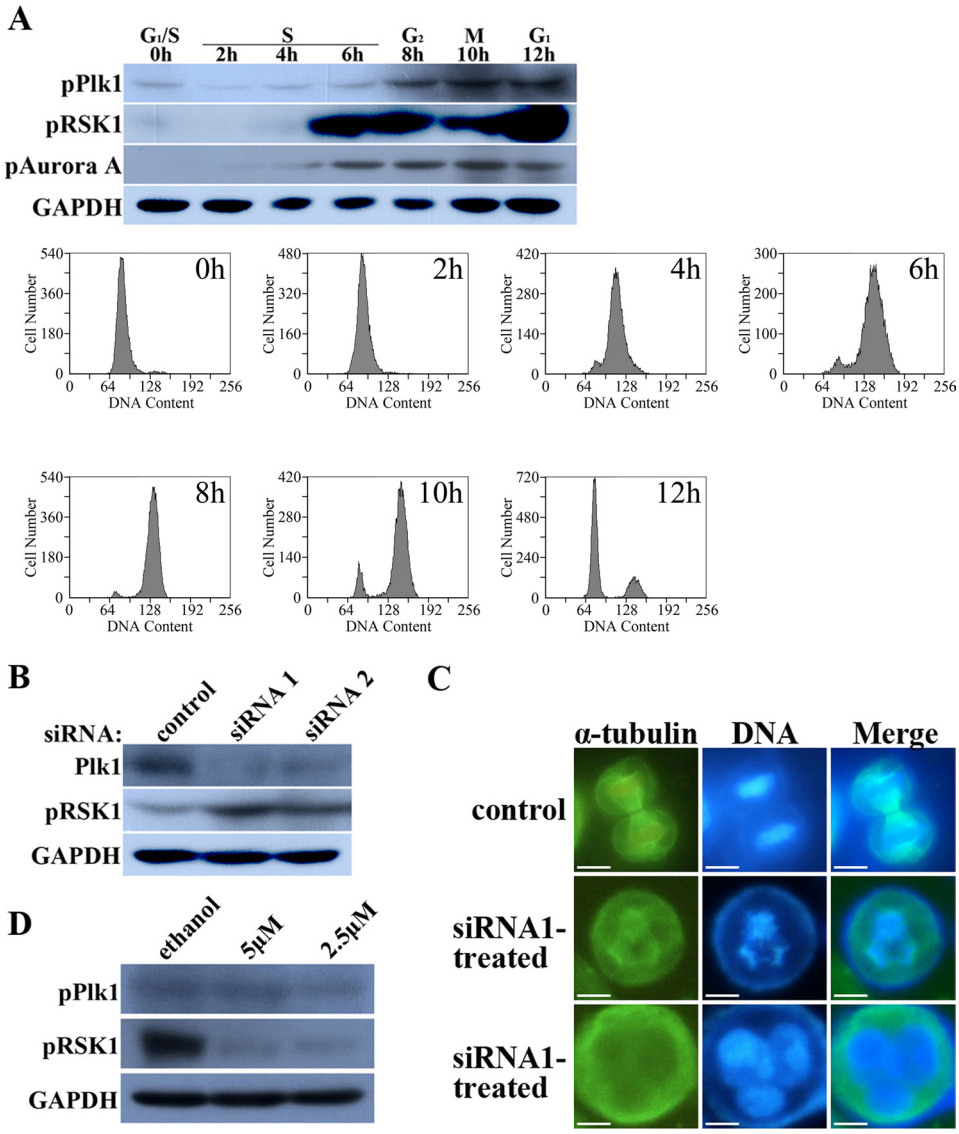

FIGURE 5. **siRNA interference of Plk1 expression in HeLa cells and treatment with specific RSK1 inhibitor.** *A*, changes in Plk1, RSK1, and Aurora A activation during the cell cycle. Analysis of cell cycle progression was performed by monitoring DNA content using flow cytometry as described under "Materials and Methods." *B*, endogenous Plk1 was successfully knocked down by both of the synthesized siRNAs, resulting in increased activation of RSK1. *C*, after treatment with Plk1 siRNA, cells exhibited an abnormal phenotype, including multiple spindle poles and multiple nuclei. *Bar*, 20 μm. *D*, treatment with the RSK1 inhibitor SL0101 (Tocris) blocked the activity of RSK1 at concentrations of 5 and 2.5 μM but did not affect the activity of Plk1.

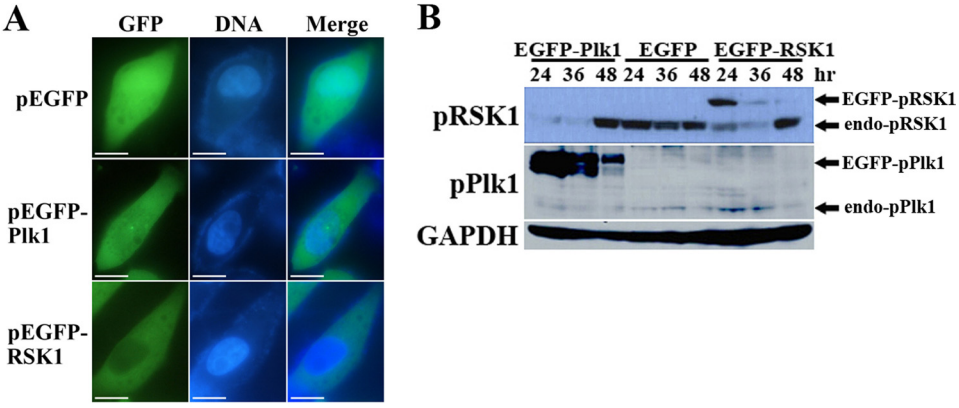

FIGURE 6. **Overexpression of *Artemia* Plk1 and RSK1 in HeLa cells.** *A*, subcellular localization of GFP-fused Plk1 and RSK1. *Bar*, 20 μm. *B*, activation of endogenous RSK1 was reduced when *Artemia* Plk1 or RSK1 was overexpressed in HeLa cells. *Black arrows* indicate activation of exogenous recombinant proteins or endogenous (*endo*) proteins. *hr*, hour; *EGFP*, enhanced GFP.

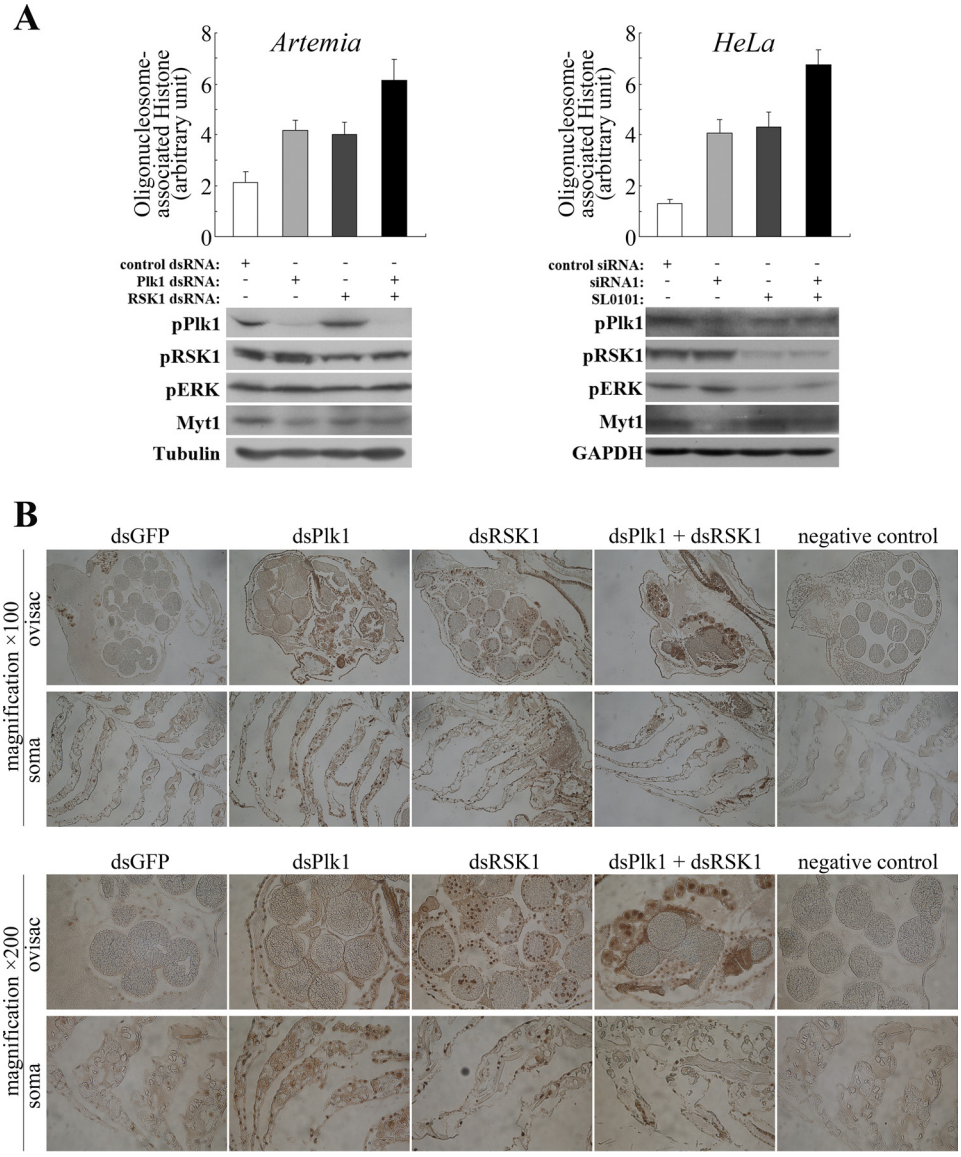

FIGURE 7. **Apoptosis detection in *Artemia* and HeLa cells upon interference with dsRNA and siRNA, respectively.** *A*, internucleosomal DNA fragmentation was quantitatively determined by detection of cytoplasmic oligonucleosome-associated histone accumulated in cells using ELISA (*top panel*). Both *Artemia* cells upon interference with dsRNAs and HeLa cells treated with siRNAs or inhibitor were analyzed (see "Materials and Methods"). Results shown represent means ± S.E. Western blot analysis of components of the Plk1 and RSK1 pathways, including Plk1, RSK1, ERK, and Myt1, in *Artemia* upon interference with dsRNAs and HeLa cells treated with siRNAs or inhibitor. α-Tubulin and GAPDH served as loading controls (*bottom panel*). *B*, apoptosis was evaluated by the TUNEL assay as described under "Materials and Methods." Representative TUNEL-stained sections from the ovisac and the soma (non-reproductive part) of *Artemia* injected with dsGFP, dsPlk1, dsRSK1, and dsPlk1 and dsRSK1, respectively. Original *magnification*, ×100 (*top panel*) and ×200 (*bottom panel*).

Plk1 RNAi group. Cell death assessment using DNA fragmentation assays showed that the somatic cells of *Artemia* upon interference with dsPlk1 and dsRSK1 undergo apoptosis (Fig. 7*A*, *top left*). Assuming that activated RSK1 in Plk1-depleted cells might contribute to the initiation of apoptosis, we used both RSK1 interference and Plk1 interference in *Artemia* and then evaluated the extent of apoptosis. If knockdown of Plk1 induced apoptosis, the reduced activation level of RSK1 should then reduce the extent of apoptosis. However, the results turned out to be just the opposite. The somatic cells in double RNAi *Artemia* exhibited more severe apoptosis than single RNAi *Artemia* (Fig. 7). Thus, these results suggested that the apoptosis induced in Plk1 RNAi *Artemia* is mainly caused by the depletion of Plk1 and not by the activation of RSK1.

As a complementary approach, a TUNEL assay was performed to evaluate DNA fragmentation, a late event in cell death by apoptosis, in *Artemia* (Fig. 7*B*). Few if any apoptotic cells were detectable in control *Artemia* injected with dsGFP. In contrast, a large number of cells undergoing apoptosis were seen in Plk1 RNAi animals. In *Artemia* injected with dsRSK1, both somatic cells and embryonic cells revealed a strong apoptosis signal. No apoptosis was seen in Plk1 RNAi embryos because they do not undergo cell division (Fig. 3). Strikingly, the somatic cells of the double RNAi *Artemia* also showed apoptosis, but its occurrence was more similar to that seen in the Plk1 RNAi group in which only somatic cells showed severe apoptosis.

To verify the effect of Plk1 and RSK1 on cell survival and to further evaluate the role of activated RSK1 in Plk1-depleted

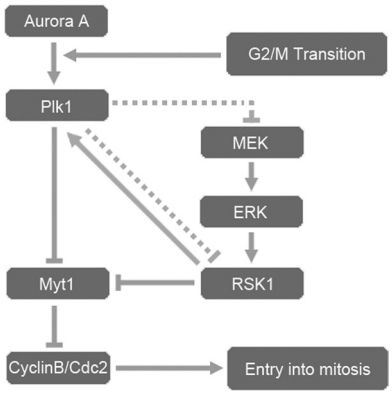

FIGURE 8. **Diagram of how inhibition of RSK1 signal pathway could occur by feedback regulation involving Plk1.** During the transition from G_2 to M phase, Aurora A phosphorylates and activates Plk1, which subsequently suppresses Myt1, the inhibitor of CyclinB/Cdc2, thereby allowing the cell to enter M phase (*gray lines*). According to this model, the MEK-ERK-RSK1 pathway can also inhibit Myt1. Plk1 is proposed to mediate the inactivation of RSK1 through upstream kinases of RSK1 or directly. In addition, exogenous expression and activation of RSK1 increases the activation level of endogenous Plk1 in a feedback-like manner. This model is tentative, and future research could lead to inclusion of other modes of action. *Dashed line*, speculated pathway.

cells, HeLa cells were treated with both the siRNA of Plk1 and the inhibitor of RSK1 to reduce the activation of these two kinases (Fig. 7*B*, *bottom right*). According to the immunoblotting results, the use of Plk1 siRNA and the RSK1 inhibitor reduced the activity of the corresponding target molecules compared with the control group. Furthermore, similar to the results in *Artemia*, double depleted HeLa cells exhibited more severe apoptosis than single treated cells, suggesting again that activated RSK1 in Plk1-depleted cells did not contribute to the activation of the apoptosis signal pathway (Fig. 7*A*, *top right*).

Fig. 8 summarizes a tentative model in highly schematic form, indicating how the Plk1 pathway might interact with the RSK1 pathway during mitosis. According to this model, during the G_2/M transition, Aurora A activates Plk1, and then Plk1 inhibits Myt1, which in turn reduces the activation of CyclinB/Cdc2, thus promoting the entry into M phase. Meanwhile, Plk1 exerts its effects on RSK1 either directly or through its upstream signal transduction pathway, MEK-ERK-RSK, causing the inhibition of Myt1 by RSK1 to be removed. In turn, the activity level of RSK1 also influences the activity of Plk1 in a feedback signal transduction mode.

DISCUSSION

In response to environmental conditions, often deleterious ones, the brine shrimp *Artemia* produces and releases encysted gastrula embryos in diapause, a state of obligate dormancy (38, 39). All cell division and DNA synthesis stop during the onset of diapause, providing a unique opportunity to study the regulation of cell cycle arrest. That cessation continues even after dormancy ends and the embryo subsequently develops into a swimming nauplius larva at which point cell division and DNA synthesis both resume (29). Thus, this system also provides the opportunity to examine the regulation of the initiation of cell division. The results of the present study show that Plk1 is involved in the formation of diapause cysts. In addition, the Plk1 signaling pathway interacts with the ERK-RSK1 pathway during different developmental stages, inhibiting activation of RSK1. Thus, Plk1 and RSK1 combine to regulate cell division and embryo development.

Many studies on these encysted embryos have focused on their extreme resistance to damaging environmental stress, ranging from severe desiccation to years of anoxia while fully hydrated at ordinary temperatures (38, 39). Understandably, a major focus has been on molecular chaperones. As one example, p26, a small heat shock protein, is expressed in very large amounts in diapause cysts and among other things is reversibly translocated into nuclei where it serves a protective function under stressful conditions like desiccation and long term anoxia (39, 40). Furthermore, in many cases, large amounts of cyst trehalose protect membranes and proteins against freezing and dehydration (41). However, the signaling pathways that induce and maintain cell cycle arrest within the cysts have remained unclear. The results of the present study showed that phosphorylation of Plk1 declined sharply in diapause cysts but increased strongly in nauplii. Because Plk1 is an essential kinase for many of the processes involved in mitosis such as centrosome maturation and bipolar spindle formation, its deactivation within cysts is consistent with cell cycle arrest just as its activation is consistent with the resumption of mitosis observed in nauplii. Consistent with these findings is that the knockdown of Plk1 in directly developing *Artemia* disrupts mitosis in the embryo, leading to the formation of pseudo-cysts.

We previously showed that RSK plays an important role in the termination of cell cycle arrest by its activation in nauplius larvae when previously arrested cells resumed mitosis (30). By contrast, RSK is not active in diapause cysts, suggesting a possible role for RSK in the initiation and maintenance of cell cycle arrest. Therefore, the interrelationship between Plk1 and RSK1 was the focus of the present study.

We found that phosphorylation of RSK1 increased significantly during the period when the oocytes remained in the ovisacs and underwent meiosis (Fig. 2), which is consistent with the important role played by RSK1 in oocyte maturation. To the contrary, high levels of Plk1 were expressed during the early stages of embryonic development but not during meiosis, findings consistent with the high protein levels of Plk1 detected during the G_2/M transition (42). The contrasting expression levels of these two kinases suggest that their functions may be interlinked. Thus, Aurora A and ERK were activated in a manner similar to that of Plk1 and RSK1, respectively, during embryonic development. Because Aurora A and ERK are upstream kinases of many signaling pathways, their changes may not fully be in accord with changes of Plk1 and RSK1. Perhaps their activation is sometimes involved with other unknown substrates. Be that as it may, one of our principal findings is that Aurora and ERK are activated before Plk1 and RSK1 activation, respectively.

According to previous research, the protein expression levels of Plk1 peak during M phase in somatic cells but remain constant during the meiotic and early embryonic cell cycles (42–45). Knockdown of Plk1 activity in *Artemia* using double-stranded RNA injections showed that phosphorylation of RSK1 increased gradually from the 1st day to the 3rd day after the oocytes entered the ovisac (uterus) in line with embryo development. In addition, the activation of RSK1 followed the acti-

vation of its upstream kinases, MEK and ERK1. This suggests that Plk1 tends to inhibit RSK1 through its upstream signal pathway (Fig. 8). Furthermore, siRNA interference of Plk1 expression in HeLa cells showed that RSK1 was phosphorylated in a similar manner. Examination of the common substrate of RSK1 and Plk1, Myt1, showed that when Plk1 was deleted activation of RSK1 occurred via an upstream RSK1 signaling pathway rather than through the simple feedback initiated by Myt1. Another interpretation is that the reduced activation level of both Plk1 and RSK1 might lead to a more severe apoptosis and less cell survival than that caused by single RNAi of Plk1. If RSK1 contributes to the death of Plk1 RNAi cells, then once RSK1 is inactivated the extent of cell death would be reduced. But our results do not support that possibility (Fig. 7). In summary, during mitosis, Plk1 has the role of inhibiting RSK1 through its upstream kinases, and this inhibition is not correlated with downstream regulation of Plk1.

Oocytes experience two rest periods during maturation. During metaphase II arrest at the end of meiosis II, cytostatic factor (CSF) is generated via mitogen-activated protein kinase (26, 46–48). Expression of Mos or MAPK causes CSF arrest (26, 49–51). Interestingly, the sole mediator of CSF arrest is p90RSK, a direct target of MAPK. In the absence of an active MAPK pathway, constitutively active RSK causes CSF arrest (52). Egg extracts depleted of RSK show no CSF activity, whereas reconstitution of RSK restores activity (53). In addition, the oocyte maturation process is only minimally inhibited by reagents that inhibit Mos synthesis or block MAPK kinase activity. This suggests that another pathway may induce maturation without the requirement for an active mitogen-activated protein kinase pathway. The polo-like kinase pathway, involved in activation of the phosphatase Cdc25C (45), is one possible alternative pathway. Therefore, the results of the present study showing that Plk1 inhibits RSK1 activity via its upstream signaling pathway are in agreement with those of previous studies and suggest that the reason that oocytes can bypass meiosis arrest and enter early mitosis is the inhibition of RSK1 by the increased expression of Plk1.

In conclusion, the results of the present study show that Plk1 regulates RSK1 activity in both *Artemia* embryos and somatic mammalian cells via the RSK1 upstream signaling pathway. These findings support the conclusion that Plk1 and RSK1 interact in a regulatory fashion during mitosis in early embryos as we describe in Fig. 8.

Acknowledgment—We are grateful to Prof. Feng-Qi Liu of the Nankai University, Tianjin, China, for the kind gift of cysts of Artemia parthenogenetica.

REFERENCES

1. Elia, A. E., Rellos, P., Haire, L. F., Chao, J. W., Ivins, F. J., Hoepker, K., Mohammad, D., Cantley, L. C., Smerdon, S. J., and Yaffe, M. B. (2003) The molecular basis for phosphodependent substrate targeting and regulation of Plks by the Polo-box domain. *Cell* **115,** 83–95
2. Johnson, L. N., Noble, M. E., and Owen, D. J. (1996) Active and inactive protein kinases: structural basis for regulation. *Cell* **85,** 149–158
3. Liby, K., Wu, H., Ouyang, B., Wu, S., Chen, J., and Dai, W. (2001) Identification of the human homologue of the early-growth response gene Snk, encoding a serum-inducible kinase. *DNA Seq.* **11,** 527–533
4. Ma, S., Liu, M. A., Yuan, Y. L., and Erikson, R. L. (2003) The serum-inducible protein kinase Snk is a G1 phase polo-like kinase that is inhibited by the calcium- and integrin-binding protein CIB. *Mol. Cancer Res.* **1,** 376–384
5. Simmons, D. L., Neel, B. G., Stevens, R., Evett, G., and Erikson, R. L. (1992) Identification of an early-growth-response gene encoding a novel putative protein kinase. *Mol. Cell. Biol.* **12,** 4164–4169
6. Bahassi, E. M., Conn, C. W., Myer, D. L., Hennigan, R. F., McGowan, C. H., Sanchez, Y., and Stambrook, P. J. (2002) Mammalian Polo-like kinase 3 (Plk3) is a multifunctional protein involved in stress response pathways. *Oncogene* **21,** 6633–6640
7. Donohue, P. J., Alberts, G. F., Guo, Y., and Winkles, J. A. (1995) Identification by targeted differential display of an immediate early gene encoding a putative serine/threonine kinase. *J. Biol. Chem.* **270,** 10351–10357
8. Xie, S., Wu, H., Wang, Q., Kunicki, J., Thomas, R. O., Hollingsworth, R. E., Cogswell, J., and Dai, W. (2002) Genotoxic stress-induced activation of Plk3 is partly mediated by Chk2. *Cell Cycle* **1,** 424–429
9. Xie, S., Wu, H., Wang, Q., Cogswell, J. P., Husain, I., Conn, C., Stambrook, P., Jhanwar-Uniyal, M., and Dai, W. (2001) Plk3 functionally links DNA damage to cell cycle arrest and apoptosis at least in part via the p53 pathway. *J. Biol. Chem.* **276,** 43305–43312
10. Eckerdt, F., Yuan, J., and Strebhardt, K. (2005) Polo-like kinases and oncogenesis. *Oncogene* **24,** 267–276
11. Takai, N., Hamanaka, R., Yoshimatsu, J., and Miyakawa, I. (2005) Polo-like kinases (Plks) and cancer. *Oncogene* **24,** 287–291
12. Gumireddy, K., Reddy, M. V., Cosenza, S. C., Boominathan, R., Baker, S. J., Papathi, N., Jiang, J., Holland, J., and Reddy, E. P. (2005) ON01910, a non-ATP-competitive small molecule inhibitor of Plk1, is a potent anticancer agent. *Cancer Cell* **7,** 275–286
13. Liu, X., and Erikson, R. L. (2003) Polo-like kinase 1 in the life and death of cancer cells. *Cell Cycle* **2,** 424–425
14. Spänkuch, B., Matthess, Y., Knecht, R., Zimmer, B., Kaufmann, M., and Strebhardt, K. (2004) Cancer inhibition in nude mice after systemic application of U6 promoter-driven short hairpin RNAs against PLK1. *J. Natl. Cancer Inst.* **96,** 862–872
15. Macůrek, L., Lindqvist, A., Lim, D., Lampson, M. A., Klompmaker, R., Freire, R., Clouin, C., Taylor, S. S., Yaffe, M. B., and Medema, R. H. (2008) Polo-like kinase-1 is activated by aurora A to promote checkpoint recovery. *Nature* **455,** 119–123
16. Seki, A., Coppinger, J. A., Jang, C. Y., Yates, J. R., and Fang, G. (2008) Bora and the kinase Aurora a cooperatively activate the kinase Plk1 and control mitotic entry. *Science* **320,** 1655–1658
17. Coleman, T. R., and Dunphy, W. G. (1994) Cdc2 regulatory factors. *Curr. Opin. Cell Biol.* **6,** 877–882
18. Nakajo, N., Yoshitome, S., Iwashita, J., Iida, M., Uto, K., Ueno, S., Okamoto, K., and Sagata, N. (2000) Absence of Wee1 ensures the meiotic cell cycle in *Xenopus* oocytes. *Genes Dev.* **14,** 328–338
19. Okumura, E., Fukuhara, T., Yoshida, H., Hanada Si, S., Kozutsumi, R., Mori, M., Tachibana, K., and Kishimoto, T. (2002) Akt inhibits Myt1 in the signalling pathway that leads to meiotic G_2/M-phase transition. *Nat. Cell Biol.* **4,** 111–116
20. Inoue, D., and Sagata, N. (2005) The Polo-like kinase Plx1 interacts with and inhibits Myt1 after fertilization of *Xenopus* eggs. *EMBO J.* **24,** 1057–1067
21. Chen, R. H., Sarnecki, C., and Blenis, J. (1992) Nuclear localization and regulation of erk- and rsk-encoded protein kinases. *Mol. Cell. Biol.* **12,** 915–927
22. Dalby, K. N., Morrice, N., Caudwell, F. B., Avruch, J., and Cohen, P. (1998) Identification of regulatory phosphorylation sites in mitogen-activated protein kinase (MAPK)-activated protein kinase-1a/p90rsk that are inducible by MAPK. *J. Biol. Chem.* **273,** 1496–1505
23. Frödin, M., and Gammeltoft, S. (1999) Role and regulation of 90 kDa ribosomal S6 kinase (RSK) in signal transduction. *Mol. Cell. Endocrinol.* **151,** 65–77
24. Palmer, A., Gavin, A. C., and Nebreda, A. R. (1998) A link between MAP kinase and p34(cdc2)/cyclin B during oocyte maturation: p90(rsk) phosphorylates and inactivates the p34(cdc2) inhibitory kinase Myt1. *EMBO J.*

17, 5037–5047
25. Ferrell, J. E., Jr. (1999) *Xenopus* oocyte maturation: new lessons from a good egg. *BioEssays* **21,** 833–842
26. Sagata, N., Watanabe, N., Vande Woude, G. F., and Ikawa, Y. (1989) The c-mos proto-oncogene product is a cytostatic factor responsible for meiotic arrest in vertebrate eggs. *Nature* **342,** 512–518
27. Watanabe, N., Hunt, T., Ikawa, Y., and Sagata, N. (1991) Independent inactivation of MPF and cytostatic factor (Mos) upon fertilization of *Xenopus* eggs. *Nature* **352,** 247–248
28. Lei, M., and Erikson, R. L. (2008) Plk1 depletion in nontransformed diploid cells activates the DNA-damage checkpoint. *Oncogene* **27,** 3935–3943
29. Nakanishi, Y. H., Iwasaki, T., Okigaki, T., and Kato, H. (1962) Cytological studies of Artemia salina. I. Embryonic development without cell multiplication after the blastula stage in encysted dry eggs. *Annot. Zool. Jpn.* **35,** 223–228
30. Dai, J. Q., Zhu, X. J., Liu, F. Q., Xiang, J. H., Nagasawa, H., and Yang, W. J. (2008) Involvement of p90 ribosomal S6 kinase in termination of cell cycle arrest during development of *Artemia*-encysted embryos. *J. Biol. Chem.* **283,** 1705–1712
31. Dai, L., Chen, D. F., Liu, Y. L., Zhao, Y., Yang, F., Yang, J. S., and Yang, W. J. (2011) Extracellular matrix peptides of *Artemia* cyst shell participate in protecting encysted embryos from extreme environments. *PLoS One* **6,** e20187
32. Nambu, Z., Tanaka, S., and Nambu, F. (2004) Influence of photoperiod and temperature on reproductive mode in the brine shrimp, *Artemia franciscana*. *J. Exp. Zool. A Comp. Exp. Biol.* **301,** 542–546
33. Dai, Z. M., Li, R., Dai, L., Yang, J. S., Chen, S., Zeng, Q. G., Yang, F., and Yang, W. J. (2011) Determination in oocytes of the reproductive modes for the brine shrimp *Artemia parthenogenetica*. *Biosci. Rep.* **31,** 17–30
34. Schmittgen, T. D., and Livak, K. J. (2008) Analyzing real-time PCR data by the comparative C(T) method. *Nat. Protoc.* **3,** 1101–1108
35. Yodmuang, S., Tirasophon, W., Roshorm, Y., Chinnirunvong, W., and Panyim, S. (2006) YHV-protease dsRNA inhibits YHV replication in *Penaeus monodon* and prevents mortality. *Biochem. Biophys. Res. Commun.* **341,** 351–356
36. Vempati, R. K., Jayani, R. S., Notani, D., Sengupta, A., Galande, S., and Haldar, D. (2010) p300-mediated acetylation of histone H3 lysine 56 functions in DNA damage response in mammals. *J. Biol. Chem.* **285,** 28553–28564
37. Hanks, S. K., and Hunter, T. (1995) Protein kinases 6. The eukaryotic protein kinase superfamily: kinase (catalytic) domain structure and classification. *FASEB J.* **9,** 576–596
38. Abatzopoulos, T. J., Beardmore, J. A., Clegg, J. S., and Sorgeloos, P. (2002) *Artemia: Basic and Applied Biology*, pp. 129–170, Kluwer Academic Publishers, Dordrecht, Netherlands
39. Clegg, J. S., Jackson, S. A., Liang, P., and MacRae, T. H. (1995) Nuclear-cytoplasmic translocations of protein p26 during aerobic-anoxic transitions in embryos of *Artemia franciscana*. *Exp. Cell Res.* **219,** 1–7
40. Liang, P., and MacRae, T. H. (1999) The synthesis of a small heat shock/α-crystallin protein in *Artemia* and its relationship to stress tolerance during development. *Dev. Biol.* **207,** 445–456
41. Crowe, J. H., Crowe, L. M., Wolkers, W. F., Oliver, A. E., Ma, X., Auh, J. H., Tang, M., Zhu, S., Norris, J., and Tablin, F. (2005) Stabilization of dry mammalian cells: lessons from nature. *Integr. Comp. Biol.* **45,** 810–820
42. Hamanaka, R., Smith, M. R., O'Connor, P. M., Maloid, S., Mihalic, K., Spivak, J. L., Longo, D. L., and Ferris, D. K. (1995) Polo-like kinase is a cell cycle-regulated kinase activated during mitosis. *J. Biol. Chem.* **270,** 21086–21091
43. Golsteyn, R. M., Mundt, K. E., Fry, A. M., and Nigg, E. A. (1995) Cell cycle regulation of the activity and subcellular localization of Plk1, a human protein kinase implicated in mitotic spindle function. *J. Cell Biol.* **129,** 1617–1628
44. Pahlavan, G., Polanski, Z., Kalab, P., Golsteyn, R., Nigg, E. A., and Maro, B. (2000) Characterization of polo-like kinase 1 during meiotic maturation of the mouse oocyte. *Dev. Biol.* **220,** 392–400
45. Qian, Y. W., Erikson, E., Li, C., and Maller, J. L. (1998) Activated polo-like kinase Plx1 is required at multiple points during mitosis in *Xenopus laevis*. *Mol. Cell. Biol.* **18,** 4262–4271
46. Gebauer, F., and Richter, J. D. (1997) Synthesis and function of Mos: the control switch of vertebrate oocyte meiosis. *BioEssays* **19,** 23–28
47. Gotoh, Y., and Nishida, E. (1995) The MAP kinase cascade: its role in *Xenopus* oocytes, eggs and embryos. *Prog. Cell Cycle Res.* **1,** 287–297
48. Singh, B., and Arlinghaus, R. B. (1997) Mos and the cell cycle. *Prog. Cell Cycle Res.* **3,** 251–259
49. Gotoh, Y., Masuyama, N., Dell, K., Shirakabe, K., and Nishida, E. (1995) Initiation of *Xenopus* oocyte maturation by activation of the mitogen-activated protein kinase cascade. *J. Biol. Chem.* **270,** 25898–25904
50. Haccard, O., Sarcevic, B., Lewellyn, A., Hartley, R., Roy, L., Izumi, T., Erikson, E., and Maller, J. L. (1993) Induction of metaphase arrest in cleaving *Xenopus* embryos by MAP kinase. *Science* **262,** 1262–1265
51. Sagata, N. (1997) What does Mos do in oocytes and somatic cells? *BioEssays* **19,** 13–21
52. Gross, S. D., Schwab, M. S., Lewellyn, A. L., and Maller, J. L. (1999) Induction of metaphase arrest in cleaving *Xenopus* embryos by the protein kinase p90Rsk. *Science* **286,** 1365–1367
53. Bhatt R. R., and Ferrell, J. E., Jr. (1999) The protein kinase p90 rsk as an essential mediator of cytostatic factor activity. *Science* 286, 1362–1365